SAND2007-0507J

Grain boundary interface roughening transition and its effect on grain boundary mobility for non-faceting boundaries

David L. Olmsted*, Stephen M. Foiles and Elizabeth A. Holm.
Sandia National Laboratories, PO Box 5800 MS 1411, Albuquerque, New Mexico 87185, USA
*e-mail: dolmste@sandia.gov

Abstract

Like other interfaces, equilibrium grain boundaries are smooth at low temperature and rough at high temperature. Very little attention has been paid to this issue, however, except in the special case of faceting boundaries. Using molecular dynamics simulations of fcc Ni, we studied roughness and mobility for two different, but closely related grain boundaries. Both boundaries are $\Sigma 5$ <100> tilt boundaries, but they have different boundary planes. In spite of their similarity, the roughening temperatures for the boundaries differ by several hundred degrees. Most importantly, the mobility of the boundaries is much greater above the roughening temperature than below. This has important implications for microstructural development during metallurgical processes.

Many engineered materials, including most metals and many ceramics and polymers, are polycrystalline; they are agglomerates of tiny, individual crystallites (grains), which are separated by internal interfaces (grain boundaries). Because grain boundaries contribute free energy to the system, there is a driving force for their removal. Thus, at high temperatures, grain boundaries move to decrease boundary area (e.g. via grain growth) or to eliminate high energy grains in favor of low energy grains. For example, grains with a magnetization vector parallel to an applied magnetic field are energetically preferred relative to those with magnetization orthogonal to the applied field; grains favorably aligned with a strain field are preferred relative to less favorably aligned grains. In both cases, given sufficient thermal energy the grain boundaries will move to eliminate the unfavored grains. The rate of grain boundary motion is governed by the boundary mobility.

Recent work has addressed the important issue of the dependence of the mobility of grain boundaries on their crystallography. Boundary crystallography is given by the angular misorientation of the neighbor grains (three degrees of freedom) and the boundary plane (two degrees of freedom)[1]. Since most experimental and computational investigations of grain boundary mobility study curved boundaries[2 3 4 5 6 7], they cannot characterize boundary plane effects or determine the absolute mobility. A few studies have investigated motion of flat boundaries under applied magnetic or mechanical driving forces,[8 9 10] obtaining the absolute mobility as a function of misorientation and boundary plane; however, these studies are limited in the boundary structures and the materials that can be accessed.

For non-faceting boundaries, boundary motion is presumed to be an activated process, so the dependence of mobility on temperature is expected to be a simple Arrhenius function. It is well known that surfaces and interfaces, including grain boundaries, undergo a roughening transition because of the competition between energy, which favors a smooth boundary, and entropy, which favors a rough one. While the behavior of a grain boundary will naturally differ between the smooth and rough states, this has typically been ignored, except in the case of faceting boundaries[1]. In this paper we show that, even for non-faceting boundaries, mobility is very different above and below the interface roughening transition. And since we also show that the roughening temperature itself can vary substantially with grain boundary crystallography, it is clear that the effect of roughness on grain boundary mobility requires more attention than it has received.

In order to study the dependence of grain boundary mobility on temperature and crystallography conveniently, we must measure the absolute mobility of flat boundaries. To achieve this, we performed molecular dynamics (MD) simulations of flat boundaries moving under the synthetic driving force developed by K. G. F Jansenns et al.[11] This method uses a classical interatomic potential and adds a potential energy to each atom that depends on the location of its nearest neighbors. If the neighbor locations are exactly, or very close to, the favored crystal A, the added energy is zero. If the neighbor locations are exactly, or very close to, the unfavored crystal B, the added energy is a fixed amount u, which in this work varies in magnitude from 0.0025 eV to 0.05 eV per atom. For positive u, system energy decreases when atoms of crystal B are converted into the orientation of crystal A. This can be achieved by moving the boundary between B and A into crystal B (or by other mechanisms, such as crystal rotation, if the system allows). While this synthetic driving force does not arise from or represent a physical driving force, it is most similar to a magnetic driving force, which in appropriate cases it could mimic.

Whether and how mobility depends on the nature of the driving force is an open question in microstructural science.[12] It is especially pertinent to these simulations, which utilize a driving force that does not arise from a physical process. To investigate how the synthetic driving force compares with a physical driving force, we compared the motion of a boundary under the synthetic driving force to motion of the same boundary under an elastic driving force, as

simulated by H. Zhang et al.[13]. Both simulations examine the same asymmetric Σ5 <100> tilt boundary with <100> and <430> boundary normals (termed boundary I) using the Voter-Chen Embedded Atom Method (EAM) potential for Ni[14], the MD method, and similar simulation cells. As shown in Figure 1, in the limit of low driving force, the synthetic driving force and the elastic driving force yield the same mobility within statistical errors. Thus, boundary motion appears independent of the origin of the applied driving force, at least in this case, and the synthetic potential method gives physically relevant results.

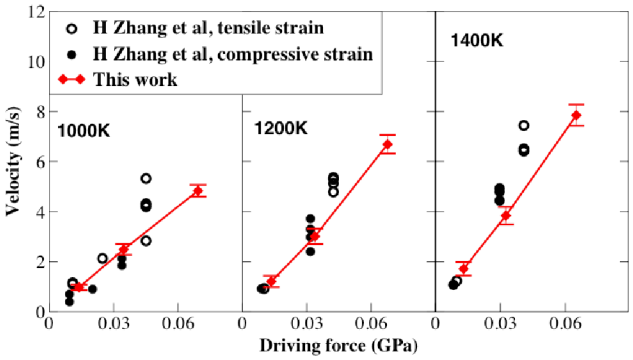

Figure 1 Velocity as a function of driving force: Ni (Voter-Chen), ∑5 <100> asymmetric tilt grain boundary with boundary normals <100><430>. In the limit of low driving force the results of the current, synthetic, driving force, and the elastic driving force of reference 13 are consistent.

One measure of boundary roughness is the standard deviation of boundary position. For periodic snapshots of our MD-generated boundaries, we measure the position of the interface in the direction normal to the interface relative to the average for that snapshot; this is often called the interface height function. Figure 2 shows the standard deviation of the interface height function averaged over all snapshots of boundary I. (Note that except for Figure 1, all results are for the Foiles-Hoyt Ni EAM potential[15].) Roughness is a function of both temperature and simulation cell size. For the largest simulation cell shown, a roughening transition occurs in the neighborhood of 900K. At this temperature, the roughness becomes non-deterministic, with some simulation runs conforming to the higher temperature data, while others line up with lower temperature data. In smaller systems no clear indicator of the transition is apparent in the roughness metric. However, even at the smallest size studied, where the boundary is approximately 35 Å by 35 Å, the results we show later exhibit a discontinuous change in the mobility at the roughening temperature.

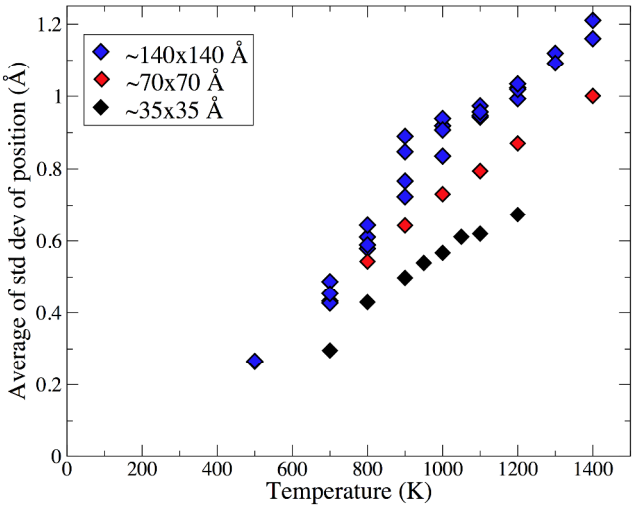

Figure 2 Roughness as a function of temperature: Ni (Foiles-Hoyt) Σ5 <100> asymmetric tilt grain boundary with boundary normals <100><430>. For the largest system size studied, a transition occurs at approximately 900K. At smaller sizes no transition is apparent. Identical symbols indicate different simulations under the same conditions.

While the key point in the current context is the existence of the transition and its temperature, notice that the spread of roughness values in Figure 2 at 900K suggests that the transition might be first order, with the potential for rough and smooth regions to coexist in the same boundary at the transition temperature. Although boundary roughening is often presumed second order, C. Rottman has suggested that long-range effective interactions between local boundary distortions can lead to a first order transition[16]. It would be interesting to perform hysteresis simulations to attempt to determine whether or not the transition is first order.

Figure 3 shows the absolute mobility (i.e. velocity divided by driving force) for boundary I as a function of temperature and driving force. Above the roughening temperature, the mobility is roughly independent of driving force and exhibits the expected Arrhenius behavior with an implied activation barrier of roughly 0.16 eV. Zhang et al. found an implied barrier of 0.26 +/- 0.08 eV for this boundary, but they included 800K data in the fit, which we believe is below the roughening transition and so should have different behavior.

For boundary I at 800K, which is below the roughening transition, Figure 3 shows that mobility decreases with driving force. Because MD is limited in the timescales it can achieve, we cannot observe very low mobilities, so we cannot measure a driving-force-independent limit for the mobility of the smooth boundary. However, we can conclude that the intrinsic mobility of the smooth boundary is much smaller than that of the equivalent rough boundary. Moreover, this effect is not a simple Arrhenius dependence on temperature, but rather reflects a change in boundary motion mechanism as the boundary structure transforms from smooth to rough.

Evidence for this change in motion mechanism is captured in Figure 4, which shows spatial trajectories for the rough (1400K) and smooth (800K) boundaries. While the rough boundary moves continuously so that its position is linear in time, the smooth boundary moves in a stepwise manner, characterized by sudden motion events interspersed with static periods of varying duration. The step size is half the lattice parameter, as expected for motion of an atomic flat boundary of this orientation. Clearly, the rough and smooth boundaries move in fundamentally different manners.

Interestingly, at high driving force, the mobility of boundary I at 800K appears to become consistent with the mobility predicted by the activation barrier derived from the higher temperature data. This suggests that the mechanism of boundary motion has become indistinguishable from that of the rough boundaries. We conjecture that the 800K boundary has become "dynamically" roughened at high driving force, but have not attempted to measure the roughness of the moving boundaries directly.

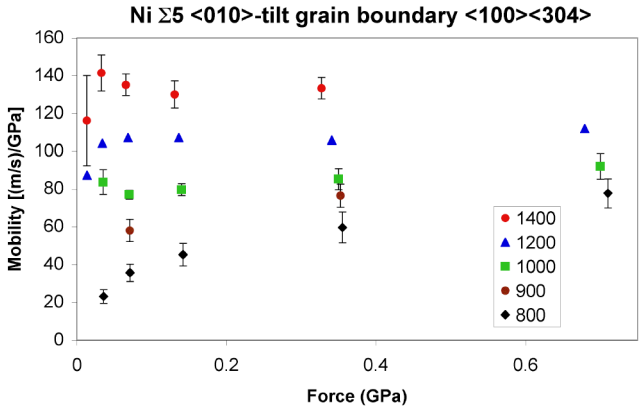

Figure 3 Mobility as a function of driving force: Ni (Foiles-Hoyt), ∑5 <100> asymmetric tilt grain boundary with boundary normals <100><430>. For temperatures of 1000K and above, the mobility is independent of the driving force within the range studied. For 800K, the mobility is similar to the high temperature mobility at very high driving force, but is substantially smaller at low driving force, and a low driving force limit is not reached at the lowest driving forces studied.

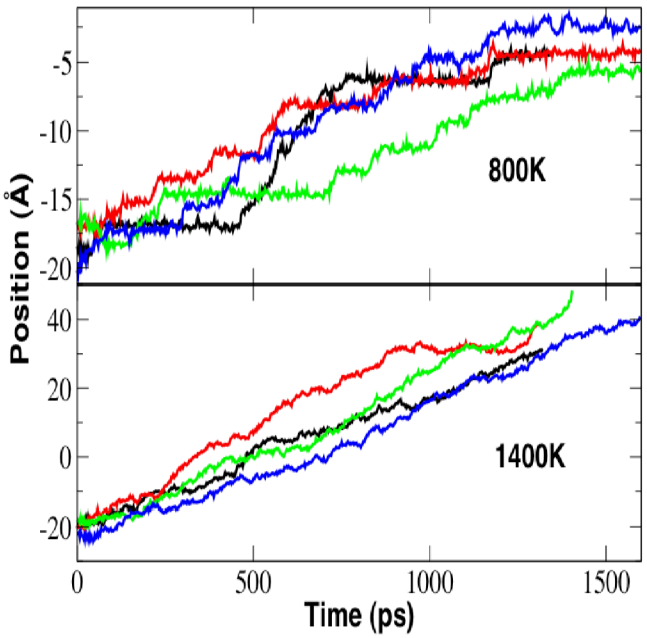

Figure 4. Motion of grain boundary I at the smallest driving force at 800K and 1400K. At 1400K the boundary is rough and moves fairly continuously. At 800K the boundary is smooth and moves in distinct steps.

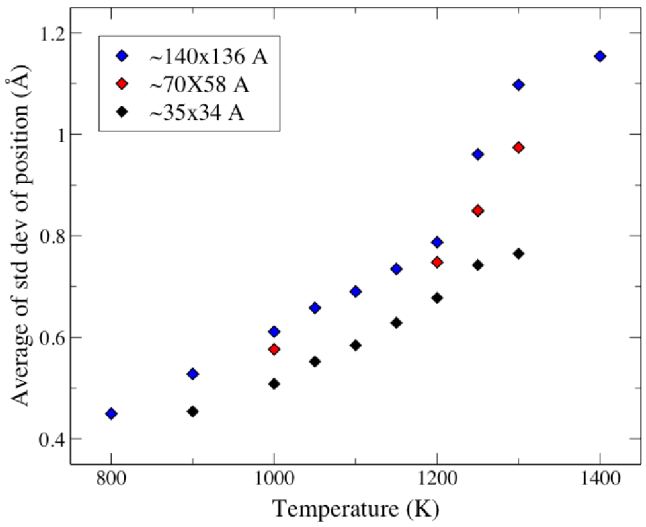

Figure 5 Roughness as a function of temperature: Ni (Foiles-Hoyt) Σ5 <100> symmetric tilt grain boundary with <310> boundary normals. For the two largest system sizes studied, a transition occurs at about 1250K.

Different behavior above and below the roughening transition has typically been studied only in faceting boundaries. However, boundary I is a general high angle boundary and should not exhibit faceting. We conclude that the difference in behavior between rough and smooth boundaries must be taken seriously for non-faceting boundaries as well. This is a primary conclusion of this paper.

Figure 5 and Figure 6 show the roughness and mobility of a symmetric Σ5 <100> tilt boundary with <310> boundary normals, which we will refer to as boundary II. This symmetric boundary is low energy, and boundaries vicinal to this one could show faceting, so it might be considered a faceting boundary in some sense. We do not observe any obvious faceting in these small systems, however.

For boundary II, Figure 5 shows a roughening transition near 1250K for the two larger system sizes studied. Notice the significant difference (~300K) in roughening temperature for boundaries I and II, which have the same misorientation and differ only in boundary plane. Because there is only one simulation for each parameter set, we cannot see "mixed" behavior at the transition temperature as we did for boundary I. Histograms of the data at the largest size suggest that the transition for boundary II is similar to that of boundary I, however.

The mobility of boundary II, shown in Figure 6, is qualitatively similar to that of boundary I. Above the roughening transition, mobility is independent of driving force and follows Arrhenius behavior. At 1000K, well below the roughening transition, mobility shows no measurable lower limit as driving force decreases but at high driving force the smooth boundary approaches the high temperature mobility. Again it appears that there is a large discontinuity in mobility between smooth and rough boundaries that is mitigated at high driving forces.

We also have simulated the other symmetric Σ5 <100> tilt boundary, which has <210> boundary normals; we term it boundary III. This boundary appears to show a roughening transition around 1250K. Well above the roughening temperature at 1400K, its mobility is independent of driving force, as in the boundaries discussed above. Slightly below the roughening temperature at 1200K, mobility decreases with driving force and dynamical roughening is observed, also as in the boundaries discussed above. However, well below the roughening transition, from 500K to 1000K, boundary mobility increases as temperature decreases, indicating a barrier-free motion subject to damping which increases with increasing temperature. (Think, for example, of dislocation mobility in the phonon-damped regime.) The increase in mobility is substantial enough that the 500K mobility is considerably higher than the 1400K mobility. In fact, the low-temperature boundary III mobility is the highest mobility we've measured for any Σ5 boundary at any temperature. This unexpected behavior appears to be related to a boundary motion mechanism involving shear[17 18], and will be discussed in another paper.

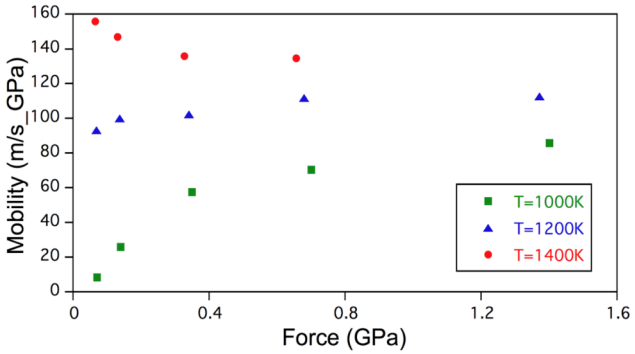

Figure 6 Mobility as a function of driving force: Ni (Foiles-Hoyt), Σ5 <100> symmetric tilt grain boundary with <310> boundary normals. For temperatures of 1200K and 1400K, the mobility is independent of the driving force within the range studied. At 1000K, the mobility is similar to the high temperature mobility at very high driving force, but is substantially smaller at low driving force, and a low driving force limit is not reached at the lowest driving forces studied.

In summary, we find that simulations of grain boundary mobility in Ni using synthetic and elastic driving forces give the same results. Thus, grain boundary mobility appears to be an intrinsic material property independent of driving force origin for these two driving forces.

A non-faceting, asymmetric Σ5 Ni grain boundary undergoes a roughening transition at 900K. Above the roughening temperature, boundary motion is continuous and mobility is high, independent of driving force, and Arrhenius in temperature. Below the roughening temperature, boundary motion is stepwise and mobility is low, decreasing with driving force, and non-Arrhenius. At high driving forces, the low temperature boundaries have mobilities consistent with rough boundary structures.

Two symmetric Σ5 Ni grain boundaries exhibit similar behavior to the asymmetric boundary, but with a roughening temperature that differs from the asymmetric boundary by 300K. Barrier-free boundary motion is observed in one case.

Computational studies of grain boundary motion often give results for activation barriers and mobilities that fail to agree with experimental results. While this is often attributed to solute effects, our results imply that the boundary roughening transition is a likely source of differences as well.

The large change in mobility at the roughening transition may have major impacts on microstructural development in polycrystalline systems. Large differences in grain boundary mobility within a single microstructure can cause abnormal grain growth[19]. At a temperature where some boundaries are smooth and others are rough, such boundary mobility differences may exist and may substantially alter the course of microstructural evolution.

Methods

The synthetic driving force used in the simulations is described briefly in the text, and in detail in reference 11. The driving forces were computed as the free energy per unit volume using thermodynamic integration of the added potential energy. The simulation cells had periodic boundary conditions for the two directions lying within the grain boundary plane. At the ends parallel to the grain boundary they had free surfaces, so that there was one grain boundary. The grain boundary was set up as a coincident site lattice boundary, and where atoms were within 1 Å of each other, the atom from one crystal was removed.

The mobilities shown are generally based on eight simulations. Four of these would have positive and four negative added potential energies, with the magnitude of the added potential energy being the same. The actual driving forces for the positive and negative added energies differ only slightly, so the average of the two has been shown. The simulation cell sizes were approximately 105 Å x 35 Å x 35 Å, with about 70 Å available for the maximum boundary motion. The simulation times were chosen to make the total motion most of the available 70 Å.

The simulations without driving force were run for 1 ns.

Acknowledgements
We thank Hao Zhang and David Srolovitz for providing the data from reference 13 shown in Figure 1 and for useful discussions.

This work was supported by the Sandia National Laboratories LDRD program and by the U.S. Department of Energy Office of Basic Energy Sciences under the Computational Materials Science Network and Core Research programs.

Sandia is a multiprogram laboratory operated by Sandia Corporation, a Lockheed Martin Company, for the United States Department of Energy's National Nuclear Security Administration under Contract DE-AC04-94AL85000.

1 Sutton A. P. & Balluffi, R. W. *Interfaces in Crystalline Materials*. Clarendon Press (Oxford, 1995).
2 Upmanyu, M., Srolovitz, D. J., Shvindlerman, L. S. Gottstein, G. Molecular dynamics simulation of triple junction migration. *Acta Mater.* **50**, 1405-1420 (2002).
3 Zhang, H., Upmanyu, M. & Srolovitz, D. J. Curvature driven grain boundary migration in aluminum: molecular dynamics simulations. *Acta Mater.* **53**, 79-86 (2005).
4 Upmanyu, M., Srolovitz, D. J., Shvindlerman, L. S. & Gottstein, G. Molecular dynamics simulation of triple junction migration. *Acta Mater.* **50**, 1405-1420 (2002).
5 Zhang, H., Upmanyu, M. & Srolovitz, D. J. Curvature driven grain boundary migration in aluminum: molecular dynamics simulations. *Acta Mater.* **53**, 79-86 (2005).
6 Adams, B.L., Kinderlehrer, D., Mullins, W.W., Rollett, A.D. & Ta'asan, S. Extracting the relative grain boundary free energy and mobility functions from the geometry of microstructures. *Scripta Mater.* **38**, 531-536 (1998).
7 Saylor, D. M., Morawiec, & A. Rohrer, G. S. The relative free energies of grain boundaries in magnesia as a function of five macroscopic parameters. *Acta Mater.* **51**, 3675-3868 (2003).
8 Zhang, H., Mendelev, M. I. Srolovitz, & D. J. "Computer simulation of the elastically driven migration of a flat grain boundary. *Acta Mater.* **52**, 2569-2576 (2004).
9 Huang, Y. & Humphreys, F. J. Measurements of grain boundary mobility during recrystallization of a single-phase aluminium alloy. *Acta Mater.* **47**, 2259-2268 (1999).
10 Winning, M., Gottstein, G. & Shvindlerman, L. S. On the mechanisms of grain boundary migration. *Acta Mater.* **50**, 353-363 (2002).
11 Janssens, K. G. F. et al Computing the mobility of grain boundaries. *Nature Mater.* **5**, 124-127 (2006).
12 Taheri, M. L, Molodov, D., Gottstein, G. & Rollett A. D. Grain boundary mobility under a stored-energy driving force: a comparison to curvature-driven boundary migration, *Z. Metallkd.* **96**[10] 1-5 (2005).
13 Zhang, H., Mendelev, M. I. & Srolovitz, D. J. Computer simulation of the elastically driven migration of a flat grain boundary. *Acta Mater.* **52**, 2569–2576 (2004).
14 Voter A. F. & Chen S. P. *Mater. Res. Soc. Symp. Proc.* **82**, 175 (1987).
15 Foiles, S. M. & Hoyt, J. J. Computation of grain boundary stiffness and mobility from boundary fluctuations. *Acta Mater*. **54**, 3351-3357 (2006).
16 Rottman, C. Phase transitions in grain boundaries with structural multiplicity. Scripta Met 23, 1037-1042 (1989).
17 Cahn, J. W., Mishin, Y. & Suzuki, A. Duality of dislocation content of grain boundaries, *Philos. Mag.* **86**, 3965–3980 (2006).
18 Cahn, J. W. & Taylor, J. E. A unified approach to motion of grain boundaries, relative tangential translation along grain boundaries, and grain rotation, *Acta Mater*. **52,** 4887–4898 (2004).
19 Holm, E. A., Miodownik, M. A., & Rollett, A. D. On abnormal subgrain growth and the origin of recrystallization nuclei. *Acta Mate*r. **51**, 2701-2716 (2003).